

6. Competing Dissociation Channels in the Photolysis of S₂Cl₂ at 235 nm

The photodissociation of disulfur dichloride (S₂Cl₂) at 235 nm has been studied by 3D imaging of the chlorine product recoil in its ground state ²P_{3/2} [Cl] and excited spin-orbit state ²P_{1/2} [Cl*] employing the resonance enhanced multi-photon ionisation and time-of-flight techniques (REMPI-TOF). The photodissociation proceeds mainly along the three channels forming S₂+2Cl (6.1), S₂Cl+Cl (6.2), and 2SCl (6.3) photoproducts where slow and fast Cl fragments are released in (6.1) and (6.2), respectively. The relative yield of channel (6.1) with respect to channel (6.2) was determined to be 1.2:1.0. The yield of Cl*, $\phi(\text{Cl}^*)=P(\text{Cl}^*)/[P(\text{Cl})+P(\text{Cl}^*)]$, was found to be 0.35. The obtained state-specific speed distributions of Cl and Cl* are mainly different in the high energy range: For Cl* the two dissociation channels are almost equally present, whereas in the case of ground state Cl the contribution of dissociation channel (6.2) is of minor importance. The dependence of the anisotropy parameter β on the fragment recoil velocity was directly determined due to the novel technique where the 3D momentum vector of a single reaction product is observed. For both spin-orbit states the anisotropy parameters differ for slow, intermediate, and fast chlorine atoms. The observed β values change from zero to slightly negative values up to positive values with increasing kinetic energy. These observations can be explained by two overlapping dissociation channels, where the two-body channel (6.2) releases the chlorine atom with high kinetic energy and a positive β parameter via an excited ¹A state, whereas the three-body channel (6.1) proceeds mainly sequentially, where the first Cl atom is released with intermediate speed and a slightly negative β value via an excited ¹B state, while the second Cl product atom in the decay of S₂Cl is released isotropically with slow recoil velocities. In addition, the dissociation energy for S-Cl bond fission was revised to be $D_0(\text{ClS}_2-\text{Cl}) = 206 \pm 7$ kJ/mol.

6.1 Introduction

The UV absorption spectrum of S₂Cl₂,¹⁻³ shown in Fig. 6.1, starts at a wavelength of 350 nm with a first maximum around 300 nm followed by a broad absorption peak at 260 nm. The broad continuum is attributed to the $n \rightarrow \pi^*_{\text{S-S}}$ and the $n \rightarrow \sigma^*_{\text{S-Cl}}$ transition,

where the non-bonding orbitals can be located at the S or the Cl atoms. Below 230 nm, another absorption band starts to rise which has not yet been assigned.² The ground state of S₂Cl₂ is of C₂ symmetry as determined by electron diffraction⁴ and is shown in Fig. 6.2.

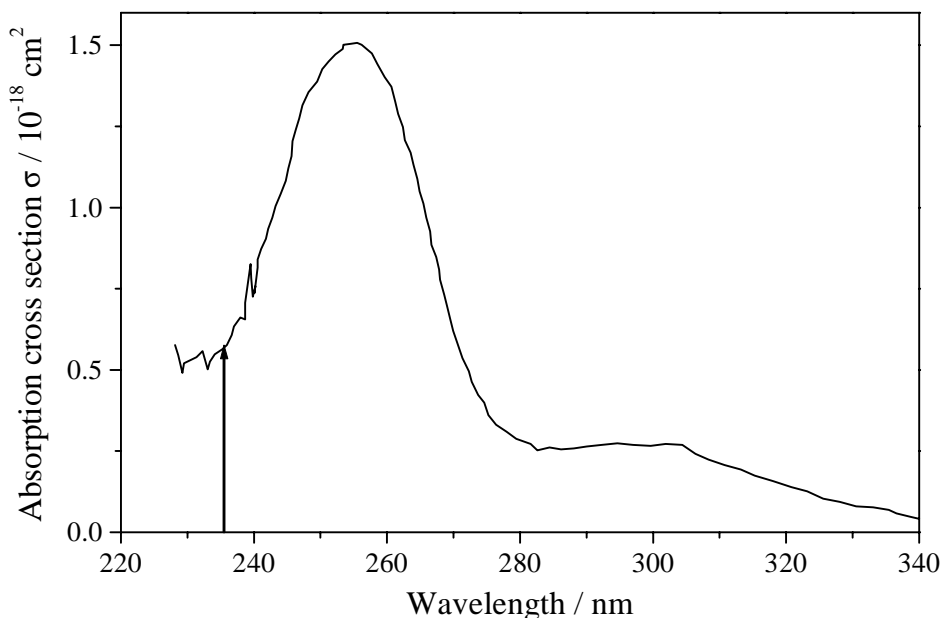


Figure 6.1: Absorption cross section of S₂Cl₂ based on the publication of Speth et al.¹ The wavelength used in the present experiment is marked by an arrow.

The photolysis of the S₂Cl₂ molecule has been the subject of several experimental investigations for decades covering the whole spectral range from 110 nm to 514 nm.⁵⁻¹¹

The following dissociation channels were observed:



Tokue et al.⁵ studied the photoabsorption cross section and the fluorescence excitation spectrum of S₂Cl₂ vapor in the range 110-200 nm using synchrotron radiation. They assigned a number of broad bands in the 120-170 nm region as Rydberg transitions. The predominant photodissociation process in the 120-155 nm region was the three-body decay (6.1),¹² where S₂Cl₂ splits into three photofragments.

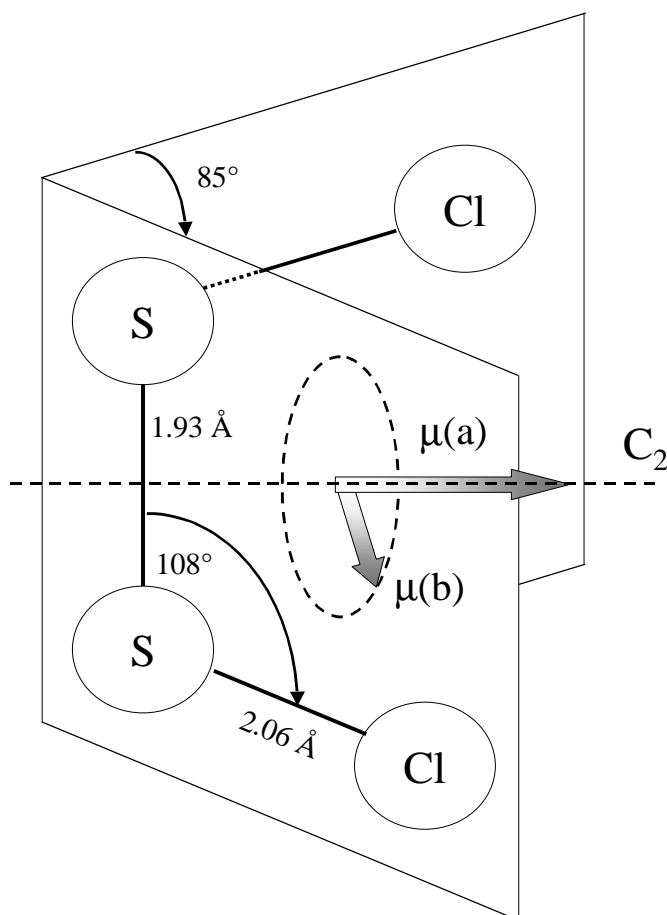


Figure 6.2: Structure² of S_2Cl_2 and the geometry of both transition dipole moments μ (a) parallel to the symmetry axis C_2 and μ (b) lying in the plane perpendicular to the C_2 axis.

At the same time Tiemann et al.⁶ studied the SCl radical generated by the photolysis of S_2Cl_2 at 248 nm by infrared diode laser spectroscopy. It was found that the photolysis yields the SCl radical in its electronic ground state via channel (6.3). Later Park et al.⁷ studied the photodissociation of S_2Cl_2 at 308, 248 and 193 nm where for the first time the radical channel (6.2) was observed. In addition, Park et al.¹³ used the photolysis of S_2Cl_2 at 248 nm as a source of Cl radicals to study the reaction dynamics of chlorine atoms with deuterated cyclohexane. The radical decay channel (6.2) was confirmed by Lee et al.⁸ by translational spectroscopy at 308 nm. It was observed that S_2Cl_2 dissociates via channel (6.2) with a mean translational energy $\langle E_T \rangle$ of 65 kJ/mol and the measured anisotropy parameter β was 0.4 ± 0.2 . Lee et al. concluded that S_2Cl_2 undergoes a fast dissociation process after excitation via a parallel transition. However, the interest in the photodissociation of S_2Cl_2 exceeded the UV region, as Chiu and Chang⁹ studied the resonance Raman and fluorescence spectra of the S_2Cl radical which was generated by the photodissociation

of S₂Cl₂ using 514.5 nm laser radiation. They confirmed that the radical channel (6.2) dominates at 514.5 nm which is also the case in the photodissociation at 308 nm.

Recent work includes two studies by Tiemann, Lee, and co-workers.^{10,11} Tiemann et al.^{1,6,10} studied the major dissociation channels of S₂Cl₂ in the range between 280 and 240 nm by using LIF and REMPI-TOF detection technique on the state-specific photofragments S and S₂. They concluded that the high-energy edge of the main absorption maximum is mainly the result of a fragmentation either into S₂+Cl₂, where Cl₂ is in the ³Π state, or into S₂+2Cl. The long wavelength part of the absorption spectrum is connected to the channel S₂Cl+Cl (6.2) and towards shorter wavelength a complex competition between different dissociation channels is expected. The involvement of SCl as an intermediate product is less favorable. In addition to the above described channel, Tiemann et al. observed the dissociation into SCl₂+S along channel (6.4).

Lee et al.¹¹ studied the photodissociation of S₂Cl₂ at 248 nm and 193 nm by translational spectroscopy. The SCl product was detected with a relative yield of 20 %. Due to the measured anisotropy parameter β_{SCl} of 1.6 at 248 nm and 0.6 at 193 nm, they concluded that a rapid S-S bond fission takes place on the excited ¹B state. Lee et al. observed that the S-Cl bond fission is predominant with a factor 3.0 higher than the S-S bond fission. Via reaction (6.2) two separate product Cl atom translational energy distributions of $\langle E_T \rangle = 42$ and 126 kJ/mol were found. The slow S₂Cl fragments undergo a secondary dissociation to form isotropically distributed S₂ and Cl which probably arise from the S₂Cl ground electronic state, whereas the fast components more likely originate from a mixed excitation of ¹A and ¹B states of S₂Cl₂. In addition, they observed the dissociation channel (6.4). At 193 nm the three-body decay channel (6.1) becomes more efficient forming S₂ and 2Cl with a Cl atom translational energy distribution of $\langle E_T \rangle = 42$ kJ/mol which is in agreement with the value derived by Park et al.⁷ However, the former interpretation given by Park that the observed Cl are released via a radical channel at 193 nm was misleading. The observed β_{Cl} value of -0.3 hints at an involvement of a higher ¹B state in the excitation.

The former studies show that the dissociation of S₂Cl₂ following absorption in the main band 230 nm and 280 nm is a highly complex process involving several excited potential energy surfaces and all decay channels (6.1) to (6.4) are in competition to each other. In

order to elucidate the dynamics behind this complicated behavior more detailed experimental data are required. Since we are able to observe the 3D momentum vector of a single state-selective photofragment by applying a novel 3D imaging technique^{14,15} the unsolved questions in the photodissociation of S₂Cl₂ are a promising task to study. There are the relative yield of the reactions, the spin-orbit branching ratio of Cl*/Cl, the translational energy disposal, the different involved upper states, and the mechanism of the decay. To this end, the energy dependence of the anisotropy parameter β is the most valuable tool to analyze the dissociation process including the dissociation energy $D_0(\text{ClS}_2\text{-Cl})$.

6.2 Experiment

A more detailed description of the experimental set-up and the novel position-sensitive detector (PSD) has been published elsewhere.^{14,15} Briefly, it consists of a combination of a home-built single-field time-of-flight (TOF) mass spectrometer and a position-sensitive detector.¹⁶⁻¹⁸ The spectrometer was evacuated to a base pressure of about 10⁻⁸ mbar by a turbo molecular pump system. Disulfur dichloride was constantly cooled to -10°C (gas pressure: about 1 mbar at -10°C) to prepare a mixture of 0.03 % S₂Cl₂ in helium which was flowing through the cooling vessel. The mixture was fed into the spectrometer via a continuous supersonic beam. With a nozzle diameter of 20 μm and a stagnation pressure of about 3 bar typical working pressures were in the order of 10⁻⁷ mbar. Under these conditions the beam is characterized by a rotational temperature of 8 K, determined by a rotationally resolved calibration spectrum of the NO (A²Σ⁺ ← X²Π) transition.¹⁴

Simultaneous dissociation and state-selective detection of chlorine atoms were performed using one dye laser pumped by a Nd:YAG laser (Coherent, Infinity 40 100). The dye laser (Lamba Physik, Scanmate) was operated with Coumarin 47 at a repetition rate of 100 Hz, its light was frequency-doubled by a BBO crystal and focussed by a 20 cm lens in order to decrease the reaction volume to 5·10⁻⁴ mm³. The energy of the frequency-doubled light was kept low (< 1 μJ) to obtain approximately one fragment signal per ten laser pulses to avoid kinetic energy transfer to the fragments due to space charge effects and saturation of the dissociation step. The laser beam, the molecular beam, and the detector axes were mutually orthogonal in the interaction region. Ultimate care was taken to overlap the light

and the molecular beam which was checked frequently by monitoring of NO via (1+1) REMPI at 226 nm and optimization of the signal intensity.¹⁹ The polarization of the laser was changed by a half wave plate in order to investigate the spatial fragment distribution. Typically the acceleration voltage was 800 V in the acceleration tube of the TOF spectrometer corresponding to an acceleration field of 16 kV/m.

The ²P_J state of the chlorine atom is split by 882 cm⁻¹ due to spin orbit-coupling into Cl(²P_{3/2}) and Cl*(²P_{1/2}). Both states were detected by a (2+1) REMPI process. The ground state was probed via the (²D_{3/2} ← ²P_{3/2}) transition at 235.336 nm, the excited state by the (²P_{1/2} ← ²P_{1/2}) transition at 235.205 nm.^{20,21} Typically the dye laser was scanned over a range of ± 0.003 nm around the Cl atom transition accounting for the Doppler broadening. Signals were digitized by time-to-digital converters (TDCs), accumulated over 2·10⁵ laser shots, and saved on-line by a personal computer. Details of the analyzing procedure are described in chapter 2.3.

The PSD includes a delay-line anode (DLA) introduced into the spectrometer chamber right behind the double stage micro-channel plates (MCPs). The PSD allows to monitor all three components of the momentum vector from the measured position of the particles on the detector and the corresponding time-of-flight (TOF). Therefore, a full 3D velocity distribution is observed and the complete information about the kinetic energy distribution and the velocity dependent β parameter can be obtained.

6.3 Results and Discussion

Upon excitation at 235 nm the photodissociation of S₂Cl₂ may proceed via different decay channels which are well characterized by Speth et al.¹ As we probe Cl and Cl* photoproducts, two decay channels will be discussed in the following, i.e. reaction (6.1) which is called the three-body decay channel and reaction (6.2) which is named radical or two-body-decay channel:



The dissociation enthalpies were calculated from the standard enthalpies of formation ($\Delta_f H^0$)²² of the molecules and radicals involved in the process and the errors were calculated according to the given errors of the individual standard enthalpies. The enthalpies were calculated for the spin-orbit ground state Cl. The ΔH^0 required for formation of one or two Cl* atoms is higher by 10.6 and 21.2 kJ/mol, respectively.

In the following five aspects characterizing the photodissociation dynamics will be discussed: the spin-orbit branching ratio, the speed distribution, the anisotropy parameter β , the maximal lifetimes of the excited states, and the translational energy disposal E_T/E_{av} via the different decay channels.

6.3.1 Spin-Orbit Branching Ratio

The spin-orbit branching ratio was obtained by scanning the laser over the two resonance transitions of Cl and Cl*. The measurements were repeated at different laser light intensities. Integrating the area S under the Doppler profiles results in a signal ratio $S(\text{Cl}^*)/S(\text{Cl})$ of 0.50 ± 0.04 . Taking the ratio of transition probabilities B of 1.06^{21} into account we determined a Cl* yield of $\phi(\text{Cl}^*) = 0.35 \pm 0.03$ where ϕ is defined as the ratio of the number of excited state atoms $P(\text{Cl}^*)$ to the total number of released chlorine atoms: $\phi(\text{Cl}^*) = P(\text{Cl}^*)/[P(\text{Cl})+P(\text{Cl}^*)]$. The branching ratios given by Tiemann et al.²³ (0.17) and Park et al.⁷ (0.21) at 248 nm are somewhat lower which is probably due to the different excitation wavelengths as Park et al.⁷ concluded that the relative yield as well as the total Cl atom production of the S₂Cl₂ molecule varied with the wavelength studied.

6.3.2 Speed Distribution

In Fig. 6.3 the speed distributions and the speed dependent anisotropy parameter β for Cl and Cl* are presented. This 1D presentation is obtained via integration of the 3D data. Cl in its ground state is mainly produced at low speeds and peaks at 1200 m/s. Only a tail is observed in the high speed region above 2000 m/s. The bimodal character is more pronounced for spin excited Cl* where the two speed regions are clearly separated. Here, the bimodal character unambiguously divides the speed distribution into two parts, where Cl* is mainly released with high kinetic energy. The speed distribution of slow Cl* atoms

which are a minor contribution peaks at 1500 m/s, whereas the peak for the fast atoms is at 2700 m/s. The small shoulder above 3600 m/s belongs to a small contribution of ^{37}Cl .

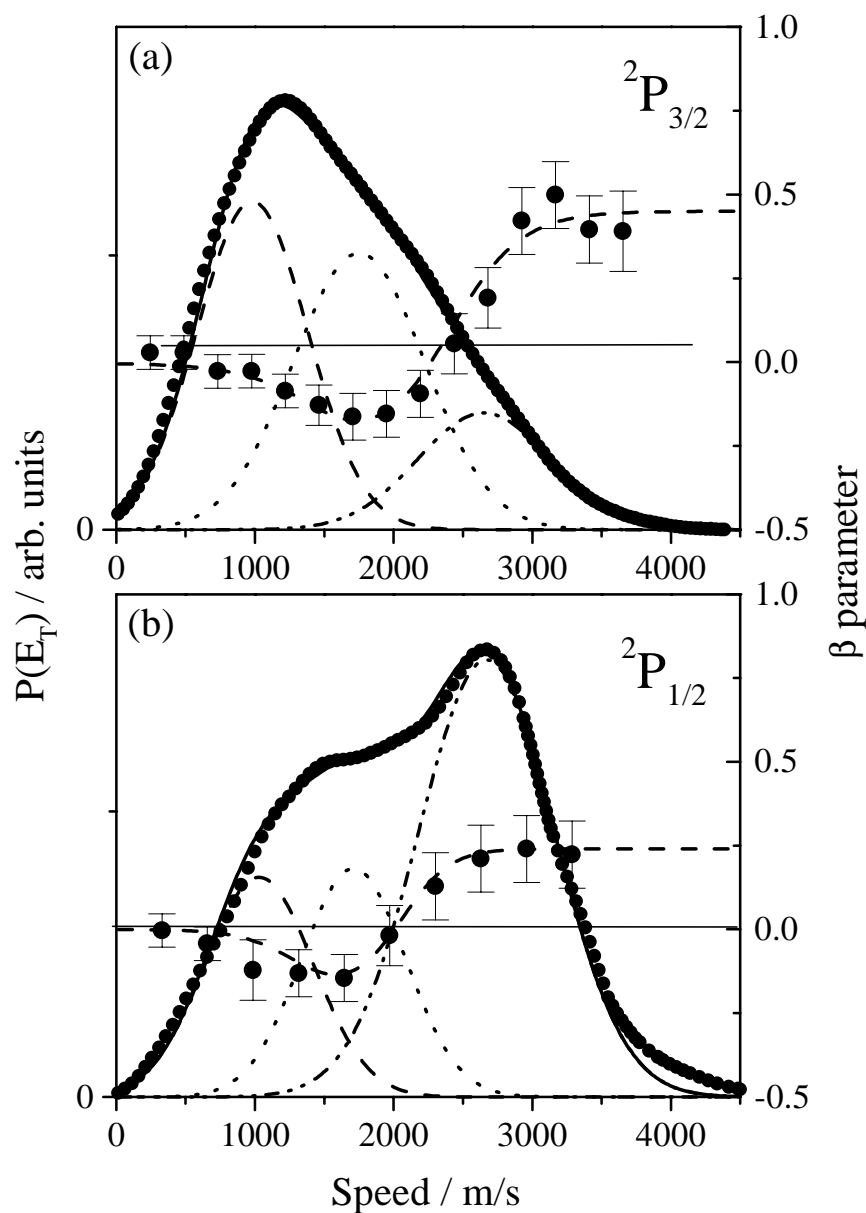


Figure 6.3: Speed distribution for (a) ground state $Cl(^2P_{3/2})$ and (b) excited state $Cl(^2P_{1/2})$ atoms produced in the photodissociation of S_2Cl_2 at 235 nm. The dependence of the β parameter on the Cl fragment kinetic energy (right scale) is shown by curves with error bars. Details of the respective high and low speed components of the trimodal distributions are listed in Table 6.1. In addition, the fit of the speed dependent β parameter (dashed line) for (a) ground state $Cl(^2P_{3/2})$ and (b) excited state $Cl(^2P_{1/2})$ to the experimentally observed data (solid circles) on the assumption of two underlying decay mechanisms. Three Gaussians were fitted to the trimodal speed distribution.

One describes the fast chlorine fragments produced in a two-body decay with a β parameter of 0.45 and 0.24 for Cl and Cl*, respectively. The other two Gaussians describe the three-body decay with a β parameter of -0.25 for the chlorine fragment released in the first step and a β parameter of zero for the slow chlorine fragment released in the second step.

The two speed regions correlate with the two different decay channels (6.1) and (6.2), where the energetic border between the two channels respective to the dissociation enthalpies is at 2250 m/s. Accordingly, the fast Cl and Cl* atoms are released via the radical decay channel (6.2) and the slow Cl and Cl* atoms are released via the three-body decay channel (6.1).

In the case of ground state Cl the contributions of the radical and the three-body decay channel are estimated to be 17 and 83 %, respectively, whereas in the case of excited state Cl* the contributions are found to be 55 and 45 % for the radical and three-body decay, respectively. Detailed information of the speed distributions for Cl and Cl* is given in Table 6.1.

Table 6.1: Characteristic data describing the speed distribution, the β parameter of the Cl and Cl* fragments and the kinetic energy release in the photodissociation of S₂Cl₂. The kinetic energy release is determined for the two- and three-body decay separately. The analysis consists of three Gaussians assuming a two-body decay (2BD) and a sequential three-body decay (3BD).

Fragments	Type	Decay channel	β Parameter	Analysis	
				Max (m/s)	FWHM (m/s)
Cl	2BD	S ₂ Cl ₂ → S ₂ Cl + Cl	0.45 ± 0.10	2650	950
	3BD	(a) S ₂ Cl ₂ → S ₂ Cl + Cl	-0.25 ± 0.07	1750	950
(b) S ₂ Cl → S ₂ + Cl		0 ± 0.05	980	800	
Cl*	2BD	S ₂ Cl ₂ → S ₂ Cl + Cl	0.24 ± 0.10	2670	980
	3BD	(a) S ₂ Cl ₂ → S ₂ Cl + Cl	-0.25 ± 0.07	1710	750
(b) S ₂ Cl → S ₂ + Cl		0 ± 0.05	1030	780	

Fragments	Type	Decay channel	E_{av} (kJ/mol)	$\langle E_T \rangle$ (kJ/mol)	$f_r = \langle E_T \rangle / E_{av}$
Cl	2BD	S ₂ Cl ₂ → S ₂ Cl + Cl	302 ¹	166	0.55 ± 0.03
	3BD	(a) S ₂ Cl ₂ → S ₂ Cl + Cl (b) S ₂ Cl → S ₂ + Cl	128	68	0.53 ± 0.03
Cl*	2BD	S ₂ Cl ₂ → S ₂ Cl + Cl	292 ¹	169	0.58 ± 0.03
	3BD	(a) S ₂ Cl ₂ → S ₂ Cl + Cl (b) S ₂ Cl → S ₂ + Cl	118	64	0.54 ± 0.03

¹ taken from the present work

6.3.3 Anisotropy Parameter β and Lifetime of the Excited State

The spatial fragment distribution $P(v, \theta) \propto f(v)(1 + \beta(v)P_2(\cos\theta))^{24,25}$ is characterized by the velocity dependent anisotropy parameter $\beta(v)$ ranging from -1 (perpendicular transition) to $+2$ (parallel transition), where θ is the angle of the polarization vector of the dissociating laser with the product recoil velocity vector, and P_2 is the second Legendre polynomial: $P_2(x) = \frac{1}{2}(3x^2 - 1)$.

The curve shape of the speed dependent β parameter has a trimodal character for both ground and excited chlorine atoms. At low velocities (< 500 m/s) the β value is close to zero, decreasing to a value of -0.15 with an increasing speed up to 1750 m/s. The β value increases strongly above 2000 m/s to a value of 0.45 ± 0.12 and 0.24 ± 0.12 for Cl and Cl*, respectively. In the case of Cl* the change from -0.15 to $+0.24$ at about 2000 m/s correlates with the determined limit in the speed distribution which divides the bimodal speed distributions in two parts. Agreeing with the above suggestion that the bimodal character in the speed distribution reflects the different decay channels, the dependence of the β values on the speed supports this view and gives us an insight in the dynamics of the photodissociation.

We will start our study for ground state Cl. At high velocities the Cl atoms have to be released via a two-body decay due to energetic reasons where the electronic transition

leads to a positive β parameter of 0.45 ± 0.12 . This positive β value suggests that the initially excited state is of ¹A symmetry, because the transition dipole moment μ for the ¹A ← ¹A transition is oriented parallel to the C₂ axis which means perpendicular to the line connecting the two S atoms and bisecting the Cl-Cl angle. The geometry and the corresponding dipole moments are shown in Fig. 6.2. A theoretical limit of 0.47 for the β parameter for instantaneous decay is estimated from the ground state symmetry with a S-S-Cl bond angle of 45.5°. If only rotation of the parent molecules is responsible for the reduction of the β parameter, the lifetime τ can be estimated based on the relationship:²⁶

$$\tau = \frac{\eta}{\omega} \quad (6.5)$$

$$\text{where } \beta_{\text{exp}} = P_2(\eta)\beta^* \text{ and } \omega = \sqrt{\frac{\pi kT}{2I}}$$

Here η is the angle between the velocity vector that would result if the molecules were not rotating and the velocity vector that actually results, ω is the angular rotational frequency, β_{exp} the experimentally observed anisotropy parameter, and β^* the theoretical limit. Assuming a molecular beam temperature of 8 K, an upper limit of the lifetime τ of 200 ± 20 fs is obtained.

In order to extract the β parameters belonging to the speed region below 2500 m/s and therefore to the three-body decay, three Gaussians were fitted to both Cl and Cl* speed distributions. As the β parameter is bimodal in the speed region below 2500 m/s, it is expected that the three-body decay occurs in a sequential way. Consequently, one Gaussian was fitted to the high speed region (> 2500 m/s), describing the two-body decay and two Gaussians were fitted to the low speed region (< 2500 m/s), describing both steps of the sequential decay: (a) S₂Cl₂ → S₂Cl + Cl and (b) S₂Cl → S₂ + Cl. The Gaussian fits are added in Fig. 6.3. The contributions of the Gaussians are used to simulate the observed curve shape of the β dependence on the speed. Since the fit functions overlap in the medium energy range, the β parameter is accordingly reduced. The obtained simulation is shown in Fig. 6.3. The best values for the β parameters are 0, -0.25, and 0.45 for ground state chlorine describing slow and intermediate Cl via three-body decay and fast Cl via two-body decay, respectively. In the case of excited state Cl* the values are 0, -0.25, and

0.24, respectively. From the negative β parameter in the low speed range it can be concluded that the three-body decay proceeds via an excited state of ¹B symmetry. The value of -0.25 is in very good agreement with former translational spectroscopy measurements at 193 nm by Lee et al.¹¹ who observed that S₂Cl₂ decays rapidly in S₂ and 2Cl with a β parameter of -0.3 on an excited ¹B state.

These observations hint at a fast dissociation, where the molecule S₂Cl₂ decays into two fragments on an excited ¹A state and mainly into three fragments on an excited ¹B state. This is supported by the overall shape of the absorption spectrum which is smooth, displaying no structure on a typical scale for vibrational spacing.¹ The continuous absorption is a good indication that direct dissociative processes take place in this region.

In the case of excited state Cl* the observed β parameter in the high speed region is 0.24 ± 0.10 . The decrease of the β parameter in comparison with the limiting value may hint at a small contribution of the excited ¹B state associated with the three-body decay releasing fast Cl* atoms. This contribution is not unlikely since a mixed excitation at 235 nm can be expected due to the location at the high-energy end of the strong absorption at 256 nm. Due to the reduction of the β parameter the contribution of fast Cl* being released via a ¹B state could be estimated to be about 6 % of the total assuming the β value of -0.25 for Cl atoms released via the ¹B state as observed for the intermediate speed Cl and Cl* atoms. Lee et al.¹¹ also favored a mixed excitation as the reason of their observed β parameter of zero for fast S₂Cl products at 248 nm. In a former study of Lee et al.⁸ S₂Cl₂ was photodissociated at 308 nm and the primary dissociation process S₂Cl₂ → S₂Cl+Cl proceeds via a slightly positive β parameter of 0.4 ± 0.2 via an ¹A state through the excitation of a ($n_{\text{Cl}} \rightarrow \sigma^*_{\text{S-Cl}}$) or ($n_{\text{S}} \rightarrow \sigma^*_{\text{S-Cl}}$) transition. Lee et al. speculated due to the existence of many nonbonding electrons in S₂Cl₂ that another repulsive ¹B state may exist. Both observations are in agreement with our present measurements. At 308 nm the Cl photoproducts were exclusively released via an excited ¹A surface yielding a positive β parameter of 0.4 ± 0.2 . The same β value is observed in the present measurement for the ground state Cl which is released solely via an ¹A state. At 248 nm Cl atoms were released via both excited states ¹A and ¹B with a positive and negative β parameter, respectively. As Lee et al. measured the averaged β parameter, a value of zero was observed. The same

value would be observed as an average at 235 nm, if there would not be the possibility to examine the speed dependence of the anisotropy parameter β .

In summary, the branching ratio of the reaction (6.1) and (6.2) was measured to be 2.45:1.0 and 0.4:1.0 for Cl and Cl*, respectively. The simultaneous absorption into the different decay channels are illustrated in Fig. 6.4 in order to emphasize the competing dissociation channels at 235 nm.

The three-body decay is found to be sequential as the second Cl atom is released isotropically with a β value close to zero, that means the intermediate S_2Cl^* lives long enough on a rotational time scale to lose the initial alignment of the parent S_2Cl_2 molecule and the second Cl atom is ejected without preferred spatial orientation.

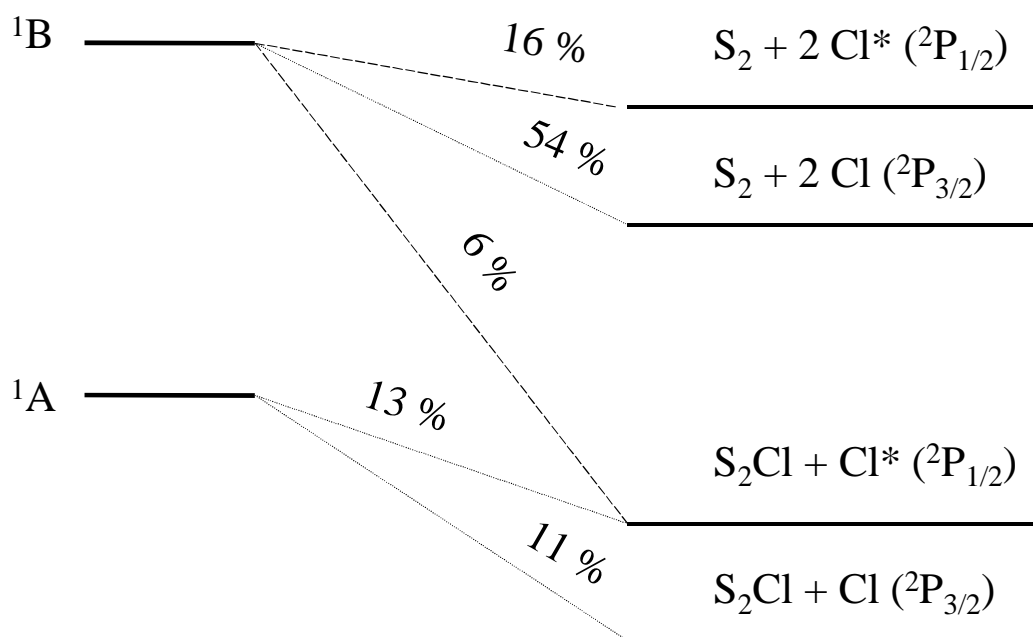


Figure 6.4: Diagram illustrating the simultaneous absorption into the excited states 1A and 1B and the different decay channels including the spin-orbit states of Cl. The contributions refer to the total number of chlorine fragments.

6.3.4 Translational Energy Disposal $\langle E_T \rangle / E_{av}$

In addition, by converting the speed distribution to translational energy distribution, the average translational energy release $\langle E_T \rangle$ of the fragment triple S₂+2Cl and the fragment pair S₂Cl+Cl can be calculated for reaction (6.1) and (6.2). For reaction (6.2), the two-body decay, the translational energy disposal $f_r = \langle E_T \rangle / E_{av}$ was determined to be $f_r = 0.55 \pm 0.03$ and $f_r = 0.58 \pm 0.03$ for Cl and Cl*, respectively. For the three-body decay reaction (6.1), the translational energy disposal fraction, $\langle E_T \rangle / E_{av}$, was determined to be $f_r = 0.53 \pm 0.03$ and $f_r = 0.54 \pm 0.03$ for Cl and Cl*, respectively. At 248 nm Lee et al.¹¹ calculated a translational energy disposal of $f_r = 0.64$ for fast S₂Cl + Cl and at 193 nm for S₂ + 2Cl $f_r = 0.54$ indicating a comparable energy disposal at 235 nm and 248 nm. An impulsive, soft radical model²⁷ would lead to a predicted translational energy disposal of $f_r = 0.65$ which is in rather good agreement with the measurements although the simple model does not take into consideration the angle dependence of the potential which can either reduce or increase the fragment angular momentum, i. e. its internal energy.^{28,29} The high kinetic energy release supports the view of a direct dissociation on a repulsive surface for both two-body and three-body decay processes.

6.3.5 Dissociation Energy $D_0(\text{ClS}_2\text{-Cl})$

Since the dissociation energy $D_0(\text{ClS}_2\text{-Cl})$ for the two-body decay (6.2) is not established in the literature with certainty, we will revise the dissociation energy from evaluating the energy balance for process (6.2):

$$\begin{aligned} E_{av} &= h\nu - D_0(\text{ClS}_2 - \text{Cl}) + E_{S_2Cl_2} \\ &= T_{S_2Cl} + E_{S_2Cl} + T_{Cl} + E_{Cl} \end{aligned} \quad (6.6)$$

where the available energy E_{av} consists of the kinetic energies T and the internal energies E of both S₂Cl and Cl fragments and is given by the sum of the photon energy $h\nu$ and the internal energy $E_{S_2Cl_2}$ of the parent molecule, diminished by D_0 . The contribution of $E_{S_2Cl_2}$ is insignificant due to the supersonic beam conditions resulting in rotational temperature

values of 8 K. The kinetic energies T_{Cl} and T_{S_2Cl} of the Cl and S₂Cl fragments are related via the conservation of linear momentum:

$$T_{S_2Cl} = \frac{m_{Cl}}{m_{S_2Cl}} T_{Cl} = \frac{35}{99} T_{Cl} \quad (6.7)$$

where m_{Cl} and m_{S_2Cl} are the fragment masses and the minor contribution of the ³⁷Cl isotope has been neglected. If it is assumed that for maximum total kinetic energy release $T^{\max} = T_{Cl}^{\max} + T_{S_2Cl}^{\max}$ no internal energy is transferred into the S₂Cl product, i.e. $E_{S_2Cl}(T^{\max}) = 0$, then for ground state Cl ($E_{Cl} = 0$) eq. (6.6) can be rewritten to yield:

$$D_0(ClS_2 - Cl) = h\nu - T^{\max} = h\nu - T_{Cl}^{\max} \left(1 + \frac{35}{99}\right) \quad (6.8)$$

In the case of electronically excited Cl* the right hand side of eq. (6.8) has further to be diminished by E_{Cl^*} . Thus, the dissociation energy $D_0(ClS_2 - Cl)$ can be determined by measurement of the maximum kinetic energy release T_{Cl}^{\max} (or $T_{Cl^*}^{\max}$) into the Cl (or Cl*) fragment. Since the maximal kinetic energy of Cl* ($T^{\max} = 292$ kJ/mol) is higher than the maximal kinetic energy of ground state Cl ($T^{\max} = 285$ kJ/mol), the dissociation energy D_0 is calculated by the former value using eq. (6.8) while taking into account the spin-orbit energy E_{Cl^*} . The obtained value for the dissociation energy $D_0(ClS_2 - Cl)$ is 206 ± 7 kJ/mol, which is in the lower energy range of the given literature value. Correspondingly, the available energy $E_{av} = h\nu - D_0(ClS_2 - Cl)$ that must be distributed onto the various degrees of freedom of both fragments, is calculated to be $E_{av} = 302 \pm 7$ kJ/mol. The low dissociation energy is supported by the observed speed and anisotropy distribution in the intermediate speed range. The observations hint also at a lower dissociation energy for the three-body decay (6.1). However, due to the overlapping decay channels, no precise determination can be performed.

6.4 Conclusions

Using 3D imaging spectroscopy, we have measured the competing dissociation channels to release S₂Cl+Cl or S₂+2Cl in the photolysis of S₂Cl₂ at 235 nm. Main experimental findings are summarized as follows:

- (1) Overall the branching ratio of the reaction (6.1) releasing S₂+2Cl and reaction (6.2) releasing S₂Cl+Cl was determined to be 1.2:1.0. If the two spin-orbit state are viewed separately, the branching ratio decreases for ground state Cl to ~2.45:1.0 and increases for excited Cl* to ~0.4:1.0.
- (2) The yield of Cl* in the excited spin orbit state ²P_{1/2} was found to be $\phi(\text{Cl}^*) = 0.35 \pm 0.03$.
- (3) The translational energy disposal for reaction (6.1) was determined to be 0.53 ± 0.03 and 0.54 ± 0.03 and for reaction (6.2) 0.55 ± 0.03 and 0.58 ± 0.03 for Cl and Cl*, respectively.
- (4) The two-body decay, releasing fast Cl (11 %) and Cl* (19 %), occurs mainly on a repulsive ¹A state through an electronic transition with a β parameter of 0.45 and 0.24 for Cl and Cl*, respectively. The reduced β value in the case of Cl* is probably due to mixed excitation of ¹A and ¹B, where 6 % of the observed Cl* are released via the excited ¹B state.
- (5) The three-body decay, releasing relatively slow Cl (54 %) and Cl* (16 %) atoms, occurs on a repulsive ¹B state through an electronic transition with a β parameter of -0.25 in the first step. The decay has a sequential character and in the second step Cl or Cl* atoms are released isotropically ($\beta = 0$).
- (6) The dissociation energy $D_0(\text{ClS}_2-\text{Cl})$ is revised to be 206 ± 7 kJ/mol.

All observations can be rationalized in terms of a simultaneous excitation on a ¹B and ¹A surface. Accordingly, the main ¹B state excitation would lead to three fragments, S₂ and

two ground-state chlorine atoms. Originally from the ¹B state, non-adiabatic coupling might be responsible for a small production of excited spin-orbit Cl atoms via two- and three-body decay. The main ¹B state excitation could be accompanied by a minor excitation of a ¹A state, fast decaying into S₂Cl+Cl, with Cl atoms generated in both spin-orbit states in almost equal amounts.

6.5 Acknowledgement

The authors are grateful to Dr. R. Aures for numerous stimulating discussions. These studies were generously supported by the Fonds der Chemischen Industrie, the Alexander von Humboldt Stiftung, and the German-Israeli Foundation (GIF). Financial support by the Deutsche Forschungsgemeinschaft is gratefully acknowledged.

-
- ¹ R. S. Speth, R. Niemann, and E. Tiemann, Chem. Phys. **229**, 309 (1998).
 - ² F. Feher and H. Münzner, Chem. Ber. **96**, 1131 (1963).
 - ³ H. P. Koch, J. Chem. Soc. 394 (1949).
 - ⁴ B. Beagley, G. H. Eckersley, D. P. Brown, and D. Tomlinson, Trans. Faraday Soc. **65**, 2300 (1969).
 - ⁵ I. Tokue, A. Hiraya, and K. Shobatake, Chem. Phys. Lett. **153**, 346 (1988).
 - ⁶ E. Tiemann, H. Kanamori, and E. Hirota, J. Mol. Spectrosc. **137**, 278 (1989).
 - ⁷ J. Park, Y. Lee, and G. W. Flynn, Chem. Phys. Lett. **186**, 441 (1991).
 - ⁸ Y. R. Lee, C. L. Chiu, and S. M. Lin, Chem. Phys. Lett. **216**, 209 (1994).
 - ⁹ C. Chiu and H. Chang, Spectrochim. Acta **A 50**, 2239 (1993).
 - ¹⁰ J. Lindner, R. Niemann, and E. Tiemann, J. Mol. Spectrosc. **165**, 358 (1994).
 - ¹¹ Y. R. Lee, C. L. Chiu, E. Tiemann, and S. M. Lin, J. Chem. Phys. **110**, 6812 (1999).
 - ¹² C. Maul and K.-H. Gericke, Int. Rev. Phys. Chem. **16**, 1 (1997).
 - ¹³ J. Park, Y. Lee, J. F. Hershberger, J. M. Hossenlopp, and G. W. Flynn, J. Am. Chem. Soc. **114**, 58 (1992).
 - ¹⁴ A. Chichinin, T. Einfeld, C. Maul, and K.-H. Gericke, Rev. Sci. Instr. **73**, N4, xxx (2002).
 - ¹⁵ T. Einfeld, A. Chichinin, C. Maul, and K.-H. Gericke, J. Chem. Phys. **116**, 2803 (2002).
 - ¹⁶ S. E. Sobottka and M. B. Williams, IEEE Trans. Nucl. Science **35**, 348 (1988).
 - ¹⁷ O. Jarutzki, V. Mergel, K. Ullmann-Pfleger, L. Spielberger, U. Meyer, R. Dörner, and H. Schmidt-Böcking, *Fast position and time-resolved read-out of micro-channel plates with the delay-line technique for single particle and photon detection*, Imaging spectroscopy IV, 322, San Diego, California (1998).

-
- ¹⁸ M. Lampton, O. Siegmund, and R. Raffanti, *Rev. Sci. Instr.* **58**, 2298 (1987).
- ¹⁹ J. Danielak, U. Domin, R. Kepa, M. Rytel, and M. Zachwieja, *J. Mol. Spect.* **181**, 394 (1997).
- ²⁰ S. Arepalli, N. Presser, R. Robie, and R. Gordon, *Chem. Phys. Lett.* **108**, 88 (1985).
- ²¹ P. M. Regan, S. R. Langfold, D. Ascenzi, P. A. Cook, A. J. Orr-Ewing, M. N. R. Ashfold, *Phys. Chem. Chem. Phys.* **1**, 3247 (1999).
- ²² M. W. Chase, NIST-JANAF, Thermochemical Tables, Fourth Edition, *J. Phys. and Chem. Reference Data*, Monograph 9, Part I + II (1998).
- ²³ E. Tiemann, H. Kanamori, and E. Hirota, *Annu. Rev.*, Institute for Molecular Science, Okazaki, Japan (1988).
- ²⁴ R. N. Zare, *Mol. Photochem.* **4**, 1 (1972).
- ²⁵ M. Mons and I. Dimicoli, *J. Chem. Phys.* **90**, 4037 (1989).
- ²⁶ G. E. Busch and K. R. Wilson, *J. Chem. Phys.* **56**, 3638 (1972).
- ²⁷ H. Okabe, *J. Chem. Phys.* **53**, 3507 (1970); *Photochemistry of Small Molecules* (Wiley-Interscience, New York, 1978).
- ²⁸ R. Schinke, *Photodissociation Dynamics*, Cambridge Monographs on Atoms, Molecular and Chemical Physics 1, Cambridge University Press, 1993.
- ²⁹ R. Aures, K.-H. Gericke, M. Kawasaki, C. Maul, Y. Nakano, G. Trott-Kriegeskorte, and Z. Wang, *Phys. Chem. Comm.* **22** (2001).